Anal. Chem. **2002,** *74,* 1642−1649

Depth Profiling of Heterogeneously Mixed Aerosol Particles Using Single-Particle Mass Spectrometry

Ephraim Woods III, Geoffrey D. Smith, Roger E. Miller,* and Tomas Baer*

Department of Chemistry, University of North Carolina, Chapel Hill, North Carolina 27599-3290

Infrared laser evaporation of single aerosol particles in a vacuum followed by vacuum ultraviolet (VUV)laser ionization and time-of-flight mass spectroscopy of the resulting vapor provides a depth profile of the particle's composition. Analyzing glycerol particles coated with 60−150-nm coatings of oleic acid using either a CO_2 laser or a tunable optical parametric oscillator as an evaporation laser results in mass spectra that depend on the IR laser power. Low infrared laser powers incompletely vaporize particles and preferentially probe the composition of the surface layers of the particle, but high laser powers evaporate the entire particle and produce spectra representative of the particle's total composition. In the limit of low laser power, the fraction of oleic acid in the mass spectra is as much as 50 times greater than the fraction of oleic acid in the particle, providing a surface-layer-specific characterization. The OPO laser provides even more surface specificity, producing an [oleic acid]/[glycerol] ratio as much as four times larger (for a 60-nm coating) than that obtained using the CO_2 laser. The infrared laser power required to sample the core of the particle increases with the thickness of the coating and is sensitive to changes in the coating thickness on the order of 10 nm. In contrast to these intuitively appealing results, high CO_2 laser powers (∼90 mJ/pulse) produce mass spectra that, at short delays between the CO_2 and VUV lasers, show enrichment of the core material rather than the coating. Likewise, tuning the OPO to frequencies that are resonant with the core material but transparent to the coating also results in selective detection of the core. The results suggest that a shattering mechanism dominates the vaporization dynamics in these situations.

The field of aerosol mass spectroscopy comprises a set of analytical techniques that are diverse in their goals and implementations, impacting both laboratory-based studies and field measurements. Many of these approaches employ lasers because of their versatility and compatibility with time-of-flight mass spectrometry.[1−8] The typical configuration employs single-laser desorption−ionization to produce a pulse of ions from each particle. Although this approach falls short of providing complete speciation, especially for organic aerosols, it has greatly broadened the scope and utility of real-time aerosol analysis. We recently introduced a two-step scheme that uses a CO_2 laser to vaporize particles and a VUV laser to gently ionize the molecules in the vapor plume. This method is better able to identify and quantify the organic components of aerosols than are single ultraviolet laser schemes.[9] The present work demonstrates that this two-step approach also provides another dimension of analysis, namely the composition of the particle as a function of the depth.

Aerosol mass spectrometry has traditionally been limited to determining the composition of particles without regard to their morphology. However, aerosol particles are not necessarily homogeneous. They may consist of multiple phases such that the core of the particle has a composition completely different from the surface layers. These "coated" particles occur, both in the laboratory and in the environment, as the result of secondary nucleation or heterogeneous chemical reactions. Specifically, recent field measurements show that many tropospheric aerosols, including sea salt particles, contain some fraction of organic matter.[1,10,11] The nearly ubiquitous organic layer is in part the result of secondary nucleation of natural organic products and organic pollutants onto the inorganic core particle. Analytical methods that distinguish these composition domains would be valuable in classifying atmospheric particles beyond their average composition. Heterogeneous chemical reactions produce coated particles when the diffusion of the reaction products in the particle is slow compared to the reaction itself, causing an enrichment of products at the surface of the particle. This process is an important consideration in laboratory measurements of the reactive uptake of gas-phase molecules by aerosol particles.[12] For both laboratory and atmospheric particles, the morphology can be an indication of the particle's history. In general, the chemical composition of the core is a reflection of the particle's origin, and the coating represents the subsequent transformations of the particle.

* Fax: (919) 962-2388. E-mails: baer@unc.edu; remiller@unc.edu.

(1) Murphy, D. M.; Thomson, D. S. *Aerosol Sci. Technol.* **1995**, *22*, 237−49.
(2) Prather, K. A.; Nordmeyer, T.; Salt, K. *Anal. Chem.* **1994**, *66*, 1403−07.
(3) Noble, C. A.; Prather, K. A. *Geophys. Res. Lett.* **1997**, *24*, 2753−56.
(4) Gard, E.; Mayer, J. E.; Morrical, B. D.; Dienes, T.; Fergenson, D. P.; Prather, K. A. *Anal. Chem.* **1997**, *69*, 4083−91.
(5) Carson, P. G.; Neubauer, K. R.; Johnston, M. V.; Wexler, A. S. *J. Aerosol Sci.* **1995**, *26*, 535−45.
(6) Mansoori, B. A.; Johnston, M. V.; Wexler, A. S. *Anal. Chem.* **1994**, *66*, 3681−87.
(7) Johnston, M. V.; Wexler, A. S. *Anal. Chem.* **1995**, *67*, 721A−6A.
(8) Neubauer, K. R.; Johnston, M. V.; Wexler, A. S. *Int. J. Mass Spectrom. Ion. Proc.* **1997**, *163*, 29−37.
(9) Woods, E., III; Smith, G. D.; Dessiaterik, Y.; Baer, T.; Miller, R. E. *Anal. Chem.* **2001**, *73*, 2317−22.
(10) Murphy, D. M.; Thomson, D. S. *J. Geophys. Res.* **1997**, *102*, 6341−52.
(11) Middlebrook, A. M.; Murphy, D. M.; Thomson, D. S. *J. Geophys. Res.* **1998**, *103*, 16475−16483.
(12) Smith, G. D.; Woods, E., III; DeForest, C. L.; Baer, T.; Miller, R. E. Submitted to *J. Phys. Chem. A.*

10.1021/ac0110909 CCC: $22.00
Published on Web 03/05/2002

Despite the importance of inhomogeneous, coated particles, they have been the subject of few aerosol mass spectrometric studies. Among the only examples of research in this area is the work of Carson et al.[13] in which they monitored in real time the deposition of an ammonium nitrite coating onto sodium chloride aerosol particles using laser desorption ionization. They found that low laser fluence detects only the surface layers of the particle, but the mass spectra at high laser fluence reflect the total composition of the particle. In this way, the surface composition may be distinguished from the total composition. The UV laser desorption ionization approach is effective in this case since photofragmentation does not inhibit the analysis. However, organic molecules fragment heavily under similar irradiances, producing mass spectra lacking in parent or structurally significant fragment ion signals. Thus, it would be difficult to identify differences in the surface and bulk compositions in organic systems using this technique. Another example is the work of Hankin and John[14] where they spatially resolve the ablation of diesel particles using a tightly focused Nd:YAG laser beam, but this technique is limited to large particles (20 μm).

Our previous work[9] demonstrates the ability of a two-laser, IR−VUV, technique to detect organic constituents of laboratory-generated aerosols with little fragmentation. The key elements of the approach are the separation of the vaporization and ionization steps, which eliminates "matrix effects", and soft ionization using a vacuum ultraviolet laser, which greatly reduces fragmentation. Similar two-step, desorption−ionization studies have been carried out using UV−multiphoton ionization rather than VUV ionization.[14,15] In cases in which the particle completely evaporates, the mass spectra quantitatively reflect the composition of the particle. In cases in which the IR laser incompletely vaporizes the particle, though, the mass spectra reflect only the portion of the particle that vaporizes. In this work, we demonstrate that incomplete vaporization followed by ionization selectively detects the outer layers of aerosol particles. Varying the power of the IR laser provides a method for establishing a depth profile of aerosol particles. In this work, we investigate glycerol particles coated with oleic acid. Glycerol is a traditional proxy for water, since it closely mimics water's solvation properties. Its low vapor pressure allows us to nucleate an oleic acid coating onto glycerol seed particles without competing with evaporation. Oleic acid, which is insoluble in both water and glycerol, is an important constituent of organic aerosols in the troposphere.

EXPERIMENT

The arrangement of the present experiment, shown schematically in Figure 1, is similar to that described in previous papers from this laboratory[9,16] and to other laser aerosol time-of-flight mass spectrometers used for on-line analysis of atmospheric aerosol particles.[1−8] The system comprises an aerodynamic lens inlet, two stages of differential pumping, a light-scattering station, and a laser-based time-of-flight mass spectrometer. Aerosol particles (2 μm in diameter) from an external gas stream enter the aerodynamic lens through a 100-μm, flow-limiting orifice. The aerodynamic lens consists of a series of orifices of successively decreasing diameter, a design based on the work of McMurry and co-workers.[17,18] The lens focuses aerosol particles onto a well-defined axis, greatly increasing the efficiency with which we detect them. The focused particles accelerate through two stages of differential pumping to speeds of ∼100 m/s before entering the chamber containing the time-of-flight mass spectrometer. The particles then pass through two 532-nm diode laser beams placed 10 cm apart. Separate photomultiplier tubes detect the scattered light from the diode lasers, and a digital timing circuit calculates the velocity of the particle on the basis of the time delay between the two scattered light signals. The circuit then triggers the pulsed lasers to fire when the particle arrives in the mass spectrometer.

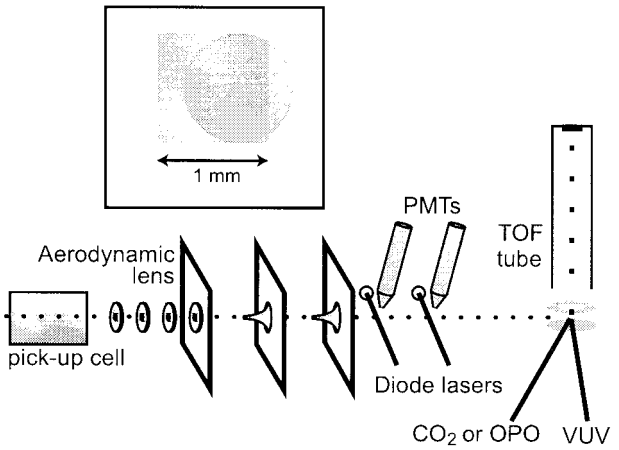

Figure 1. Schematic diagram of the experimental apparatus. It consists of an aerodynamic lens inlet, two stages of differential pumping, a light-scattering station for particle sizing and laser timing, and a time-of-flight mass spectrometer. The inset shows the spatial overlap of the CO_2 and VUV lasers.

We employ a two-laser analysis of the aerosol particles, separating the desorption and ionization steps that typically occur in a single laser pulse in other methods. Either a pulsed TEA−CO_2 laser (Lumonics) producing 15−100 mJ/pulse of radiation near 10.6 μm or a tunable Nd:YAG laser-pumped optical parametric oscillator (OPO) vaporizes the particle prior to ionization. The focal spot size for both of these lasers is ∼1 mm^2. After a delay of 2−30 μs, a 118.5-nm laser beam produced by frequency-tripling 10 mJ of the 355-nm output of a Nd:YAG laser (Continuum) in a mixture of Xe and Ar gas ionizes the vapor cloud for time-of-flight mass analysis. The main chamber and the Xe cell are coupled by a LiF lens that recollimates the 355-nm light and loosely focuses the copropagating 118.5-nm light into the chamber. We calculate a spot size of 1 mm^2 for the VUV laser on the basis of the position of the 355-nm focus in the Xe cell and the curvature of the LiF lens. The unfocused, residual 355-nm light does not appear to contribute to the signals we observe. The position of the VUV laser focus is offset from the CO_2 laser focus by a variable distance of 0.25−1 mm along the particle beam axis to account for the motion of the particle center of mass, as shown by the inset of

(13) Carson, P. G.; Johnston, M. V.; Wexler, A. S. *Aerosol Sci. Technol.* **1997**, *26*, 291−300.
(14) Hankin, S. M.; John, P. *Anal. Chem.* **2001**, *71*, 1100−04.
(15) Morrical, B. D.; Fergenson, D. P.; Prather, K. A. *J. Am. Soc. Mass Spectrom.* **1998**, *9*, 1068−73.
(16) Woods, E., III; Dessiaterik, Y.; Miller, R. E.; Baer, T. *J. Phys. Chem. A* **2001**, *105*, 8273−80.
(17) Liu, P.; Ziemann, P. J.; Kittelson, D. B.; McMurry, P. H. *Aerosol Sci. Technol.* **1995**, *22*, 293−313.
(18) Liu, P.; Ziemann, P. J.; Kittelson, D. B.; McMurry, P. H. *Aerosol Sci. Technol.* **1995**, *22*, 314−24.

Figure 1. We found that absolute shot-to-shot intensity fluctuations are only about 15%, likely due to power fluctuations in VUV intensity.

We created oleic acid-coated glycerol particles using two techniques. In the first, we nebulized a dilute mixture of both oleic acid and glycerol in 2-propanol and allowed the 2-propanol solvent to evaporate. Since the glycerol and oleic acid are mutually soluble in 2-propanol (in low concentration) but insoluble in one another, a phase separation occurs, leaving the lower surface tension oleic acid on the surface of the particle. The advantage of this technique is that it creates particles of known composition; however we found this technique reliable only for creating thin coatings. For example, a 5:1 mixture of glycerol and oleic acid produces a 60-nm coating on a 2-μm particle. In the second method, pure glycerol particles entrained in a ~1 L/min flow of Ar pass through a "pick-up" cell that contains vapor supersaturated with oleic acid, producing a coating of oleic acid on the glycerol particles. Varying the temperature of the liquid oleic acid in the bottom of the pick-up cell changes the partial pressure of the oleic acid vapor in the cell and, thus, determines the average thickness of the coating. The particles generated in this arrangement have an average total diameter of 2 μm, and an average coating thickness that varies between 100 and 150 nm, depending on the temperature in the pick-up cell. We estimate the average coating thickness for these particles by examining the total ion signals from the completely evaporated particle and by assuming that glycerol and oleic acid have similar 118-nm ionization cross sections. Although the absolute cross sections are unknown, we can measure their relative cross sections by measuring the signal intensities from completely evaporated mixed particles of known composition (such as those created by the nebulizer). Because it is difficult to ensure that our aerosol particles are completely evaporated and that the vapor is completely contained in the ionization volume, the relative cross section could be different by a factor of ~2. In the data presented here, it is the trend in the mass spectra with respect to laser power that is critical and not the absolute thickness of the coating.

Two separate observations ensure that the particles have the coated morphology. First, monitoring the composition of the aerosol particles mass spectrometrically at high CO_2 laser fluence (such that the entire particle evaporates) verifies that the supersaturation ratio in the cell is insufficient to nucleate homogeneously any pure oleic acid particles. Since homogeneous nucleation is not possible and no pure oleic droplets exist, the mixed particles created by the pick-up cell are unlikely to be composed of separate glycerol and oleic acid droplets joined at a point of adhesion. Second, we measure the threshold CO_2 laser power for detecting glycerol in the mixed particles. Figure 2 shows the integrated glycerol signal in the aerosol mass spectra for several coating thicknesses as a function of CO_2 laser power. As expected, the threshold CO_2 power for detecting glycerol increases with the thickness of the oleic acid coating, because more energy is required to remove the coating. The plot also shows the corresponding behavior for a pure (uncoated), 2-μm glycerol particle. Clearly, as the coating thickness increases, more CO_2 laser energy is required to produce a given glycerol signal intensity. If the particles were not coated (i.e., if the glycerol surface were exposed to the vacuum), we would expect that the threshold for detecting glycerol would remain constant. These data are direct evidence of the coated morphology.

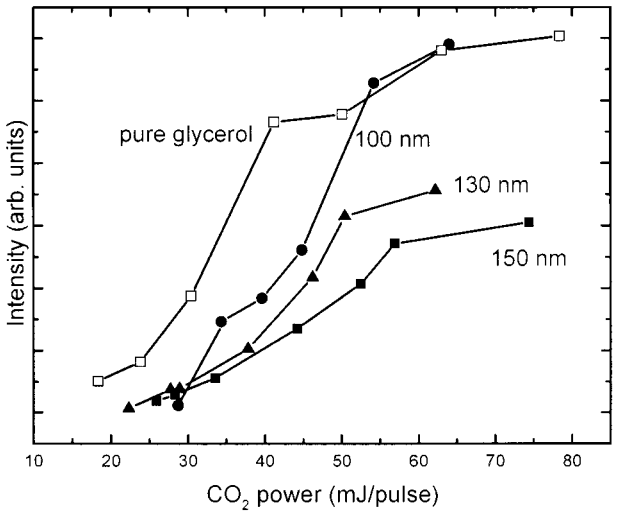

Figure 2. Integrated intensity of glycerol features in the mass spectra plotted as a function of the CO_2 laser power for pure glycerol and glycerol coated with three different thickness: 100, 130, and 150 nm.

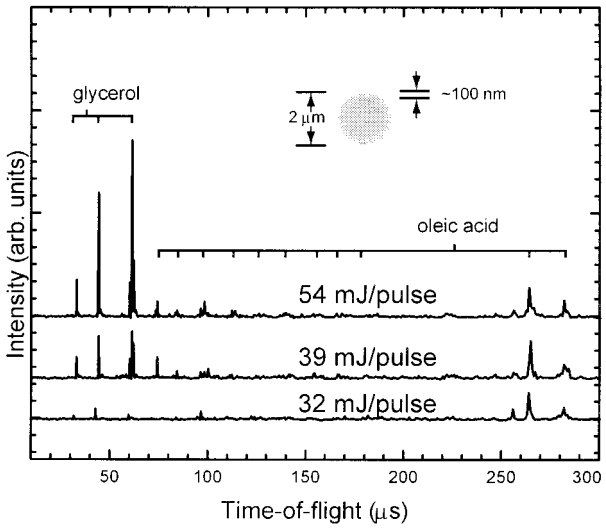

Figure 3. Mass spectra that result from analyzing 2-μm (total)-diameter particles with an average oleic acid coating thickness of 100 nm using CO_2 laser evaporation. The three traces represent three different CO_2 laser powers: 32, 39, and 54 mJ/pulse. The fraction of the signal attributable to glycerol increases with increasing laser power.

RESULTS

CO_2 Laser Evaporation. Figure 3 shows the mass spectra that result from analyzing 2-μm oleic acid-coated glycerol particles generated using the pick-up cell at three different CO_2 laser powers. We estimate the average coating thickness for these particles to be 100 nm. Each of the traces in Figure 3 represents cases in which the particle is *incompletely* evaporated. At the lowest CO_2 laser energy of 32 mJ/pulse, the predominant features in the mass spectrum arise from the parent ion of oleic acid (m/z = 282) and its two highest-mass fragment ions (m/z = 264, 256). Although glycerol accounts for about 70% of the total volume of the particle, the glycerol features (m/z = 74, 61, 44, 33) in the

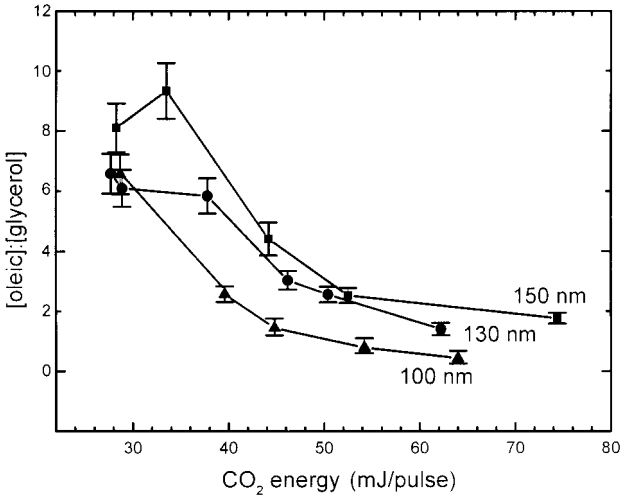

Figure 4. The [oleic acid]/[glycerol] ratio plotted as function of CO_2 laser power for three coating thicknesses: 100, 130, and 150 nm.

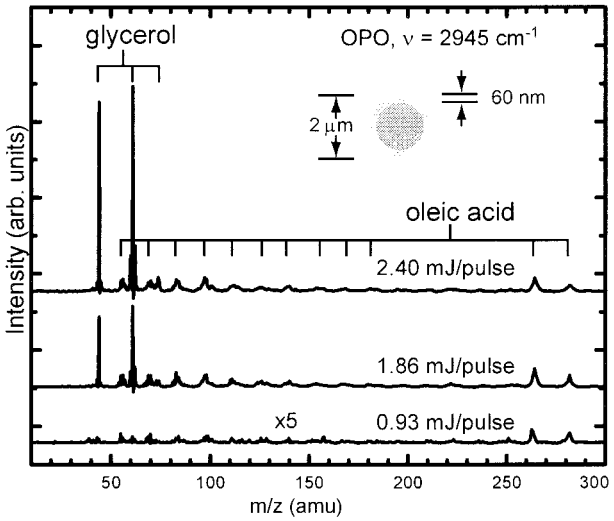

Figure 5. Mass spectra that result from analyzing 2-μm (total)-diameter particles with an average oleic acid coating thickness of 60 nm using OPO laser evaporation (2945 cm^{-1}). The three traces represent three different OPO laser powers: 0.93, 1.86, and 2.40 mJ/pulse. The fraction of the signal attributable to glycerol increases with increasing laser power.

mass spectrum account for <15% of total ion signal under these conditions. Clearly, at this low laser power, the vapor comes preferentially from the coating rather than the core. The middle and upper traces of Figure 3 show the results of the analysis for CO_2 laser energies of 39 and 54 mJ/pulse, respectively. In each case, the intensity of the oleic acid signal is nearly constant, but the glycerol signal increases with increasing CO_2 laser power.

In the case of this binary aerosol, calculating the ratio of oleic acid to glycerol intensities in the mass spectra as a function of the CO_2 laser power provides a quantitative description of the analysis. In an ideal scenario in which the vaporization laser strips away the liquid from the surface layer by layer, the [oleic]/[glycerol] ratio would be infinite at low powers and asymptotically approach some finite value that reflects the volume ratio for the entire particle. Figure 4 shows the experimental results for glycerol particles coated with three different average thicknesses of oleic acid: 100, 130, and 150 nm. In each case, the ratio is large at low CO_2 energies and drops as the CO_2 power increases. The smallest CO_2 fluence produces a ratio of ~8, which is a factor of ~40 larger than the total volume ratio for those particles. For the thinnest coating of 100 nm, the ratio drops immediately as the CO_2 laser power increases and falls monotonically to 0.3 at 64 mJ/pulse. The behavior for the two thicker coatings suggest that the CO_2 laser does not evaporate the entire oleic acid coating at the lowest CO_2 laser fluence.

The presence of small amounts of glycerol signal even at the lowest power causes the [oleic acid]/[glycerol] ratio to be finite rather than infinite and indicates that the ideal scenario described above is not met. There are two possible explanations for this behavior. First, the variability in the individual single particle spectra suggests a broad distribution of oleic acid coating thicknesses for a particular average thickness. The detection of glycerol may be completely attributable to the small fraction of particles having very thin coatings. Second, there may be contribution from an evaporation mechanism that efficiently vaporizes core molecules. We address this possibility in more detail in the Discussion section. As we will show, there is direct evidence for such a mechanism at higher laser fluence. However, at this time, we cannot distinguish between these two possibilities for the lowest laser fluences. Nonetheless, these trends in the data indicate a strong correlation between the CO_2 laser power and the depth of the analysis. Taken together with the glycerol threshold measurements in Figure 2, these observations show that depth-profiling is possible using laser vaporization. From the results in Figure 4, we estimate that the technique is sensitive to changes in the coating thickness of ~10 nm for these 2-μm particles.

OPO Laser Evaporation. To test the effect of the laser pulse parameters, we performed experiments similar to the ones described above using an optical parametric oscillator (OPO) as the evaporation laser. The CO_2 laser pulse (λ = 10.6 μm) is a typical TEA pulse, consisting of a sharply peaked portion with a duration of ~250 ns, followed by a broad emission over >1 μs. Each component of the pulse accounts for roughly one-half of the total intensity. On the other hand, the OPO laser has a Gaussian temporal profile with a width of ~5 ns. The 200-fold difference in pulse duration between the lasers results in large differences in the heating rate of the particles. Another difference is that the OPO is tunable over a wavelength range that includes the strong C−H stretch absorption bands (3.3 μm), ensuring that the particle absorbs a large fraction of the OPO radiation, as compared to the CO_2 laser beam. In addition, the wavelength of OPO radiation is similar in magnitude to the diameter of the aerosol particle, making Lorentz−Mie focusing of the infrared light within the particle more important. The resonance and focusing properties of the OPO radiation and their effect on the evaporation dynamics are discussed in more detail in the Discussion section.

Figure 5 shows the mass spectra obtained from analyzing an oleic acid-coated glycerol particle using the OPO as an evaporation source. In these experiments, the wavelength of the OPO is set to 3.39 μm (2945 cm^{-1}), which is resonant with the C−H stretching excitation in both oleic acid and glycerol. We use only a few millijoules per pulse from the OPO laser; therefore, a smaller fraction of the particle evaporates. As a result, we demonstrate the evaporation dynamics in this case using only a 60-nm coating of oleic acid. We prepared these particles from a dilute mixture

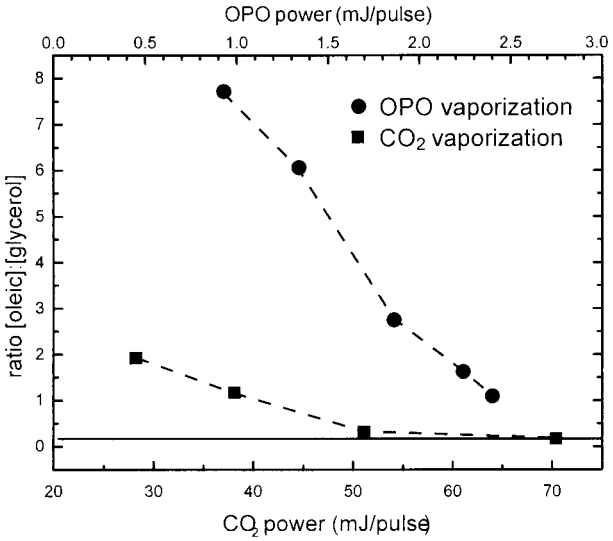

Figure 6. Comparison of the [oleic acid]/[glycerol] ratio for CO_2-laser evaporation (■) and OPO-laser evaporation (●). The horizontal line at the ratio of 0.2 represents the total volume ratio of the particle.

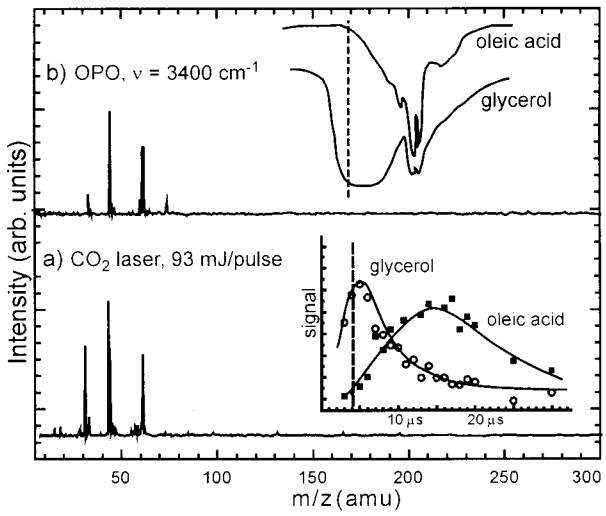

Figure 7. (a) Spectrum obtained from analyzing oleic acid-coated glycerol particles using the CO_2 laser at 93 mJ/pulse. The inset of (a) shows the CO_2−VUV delay dependence of both the glycerol (○) and the oleic acid (■). (b) Mass spectrum that results from analyzing coated particles with the OPO laser tuned to 3400 cm^{-1}. The inset of (b) shows the absorption spectrum for oleic acid and glycerol in this region of the spectrum. Both mass spectra are dominated by glycerol features.

of glycerol and oleic acid in 2-propanol using a nebulizer. A 5:1 ratio of glycerol to oleic acid in the solution produces a coating ~60 nm thick on a 2-μm particle. Similarly to the results in Figure 2 for the CO_2 laser vaporization, Figure 5 shows that the intensity of glycerol features in the mass spectra increases with increasing OPO power. Again, this behavior demonstrates that low evaporation laser fluences preferentially probe the surface layers of the particle.

A comparison of the spectra obtained using the OPO to those obtained using the CO_2 laser shows that OPO vaporization is the more surface-specific technique of the two. Figure 6 is a plot of the [oleic acid]/[glycerol] ratio as a function of the evaporation laser power for both OPO and CO_2 laser evaporation of the particles with a 60-nm coating. For the CO_2 laser at 28 mJ/pulse, the lowest power that produces an adequate signal, the ratio is ~2. However, for the OPO at 0.93 mJ/pulse, the ratio is nearly 8. As we alluded to earlier, the pulse parameters (including the relative extinction) of the OPO laser are quite different from the CO_2 laser parameters, and this difference results in an increased surface specificity for the OPO analysis of these particles. Both traces converge to the value, 0.2, that is representative of the total volume of the particle (assuming that the VUV laser ionizes the glycerol and oleic acid molecules with equal efficiency). In fact, the CO_2 laser trace reaches that ratio at just above 70 mJ/pulse, suggesting that the particle is nearly completely evaporated with that laser fluence.

Selective Detection of the Core. The previous section describes cases in which the evaporation laser produces a depth-sensitive analysis. In this section, we will explore conditions in which the composition of the particle's core is detected preferentially. Figure 7a shows the mass spectrum that results from analyzing oleic acid-coated glycerol particles (2-μm total diameter with 60-nm coating) using the CO_2 laser at 93 mJ/pulse, a larger laser power than shown previously. At the CO_2−VUV laser delay used here (2 μs), glycerol features dominate the spectrum, with the oleic acid features totaling <5% of the total intensity. The fraction of oleic acid in the particle is >19%; therefore, the mass spectrum represents a much *lower* fraction of oleic acid than one would expect even from a completely evaporated particle. Therefore, the vapor created by the CO_2 laser comes preferentially from the core of the particle in this example. This result suggests that it is possible to evaporate molecules in the core while leaving coating molecules in the condensed phase, a counterintuitive result given the morphology of the particle. The inset of Figure 7a, which plots separately the integrated signal for oleic acid and glycerol as a function of the CO_2−VUV delay, helps elucidate these dynamics. The glycerol vapor appears quickly, causing the mass spectra at short delay to favor glycerol. Oleic acid appears more slowly and dominates the spectra at longer delays (>10 μs). In the depth-profiling regime, the delay dependence of both the glycerol and oleic acid signals are very similar to the oleic acid signal in the present case. That is, the vapor appears over a period of about 10 μs and decays slowly, with the ratio of glycerol to oleic acid ratio remaining nearly constant. Here, the peak glycerol signal is shifted to much shorter delays (<5 μs) than in the depth-profiling regime. The drastic shift in the optimum delay for detecting glycerol molecules in the high-power case indicates a new evaporation is operative. We conclude that the CO_2 laser shatters the particle into several smaller, oleic acid-rich particles plus some vapor that originates predominantly from the parent particle's core of glycerol. In this case, the resulting nanoparticles are warm enough to undergo further evaporation (aided by the long CO_2 laser pulse), and this process produces the oleic acid signal at longer delay.

We also observed a preferential detection of core molecules in the (much lower power) OPO + VUV experiments when the wavelength of the OPO is resonant with core (glycerol) molecules but not with coating (oleic acid) molecules. Figure 7b shows the mass spectrum from the OPO + VUV analysis with the OPO wavelength set to 2.94 μm (3400 cm^{-1}), which is resonant with the O−H stretch of glycerol, and with an OPO−VUV delay of 10 μs. The inset of Figure 7b shows the IR absorption profiles of oleic acid and glycerol in the region of the O−H and C−H

stretches. The dotted vertical line indicates the wavelength (2.94 μm) at which we performed the experiment. Although oleic acid constituted 19% of the particle, oleic acid features accounted for only 1% of the integrated intensity in the spectrum. In this case, we did not observe appreciable oleic acid evaporation, even at longer delays. Again, shattering may be responsible for generating vapor from the core of the particle and not from the coating, as thermal (layer-by-layer) or ablative evaporation would produce vapor from the coating as well. We discuss this shattering mechanism further in the following section.

DISCUSSION

Depth Profiling. The data presented here demonstrate the ability of a two-laser analysis to provide a profile of composition vs depth of aerosol particles. For the 2-μm aerosol particles used in this study, the depth profile is sensitive to changes on the order of 10 nm in the coating thickness. This is the first such result for aerosols containing organic constituents, which are so prevalent in the troposphere. Interpreting these data requires knowledge about the mechanism of evaporation generated by the CO_2 and OPO lasers. Several recent articles address the effects of the laser pulse parameters on the mechansim of laser desorption in bulk solids and aerosols.[19−22] Most laser desorption processes occur in the limit of thermal confinement.[22] This condition arises when the laser pulse duration, τ_p, is shorter than the time for thermal equilibration, $\tau_{th} \sim L_p^2/D_T$, where L_p is the size of the absorbing structure (the aerosol particle) and D_T is the thermal diffusivity of the material. Since τ_{th} is on the order of 10 μs, and τ_p is $\leq$1 μs for the 2-μm particles used in this study, the limit of thermal confinement applies to both CO_2 and OPO laser desorption. As a result, the IR laser may heat the particle well beyond its normal boiling temperature. The evaporation dynamics change from a purely surface evaporation at low laser fluences to an explosive evaporation, or phase explosion, of the superheated particle at high fluences. According to matrix-assisted laser desorption experiments and molecular dynamics (MD) simulations,[23,24] as well as fast photography of exploding droplets,[25] laser-initiated, explosive vaporization in this heating regime results in the creation of both nanodroplets and vapor. It has been suggested that a normal boiling mechanism is relatively unimportant in laser desorption, because the diffusion of bubbles is slow compared to the dynamics of explosive vaporization.[21] Another possible limit is that of inertial, or stress confinement, which may be designated as $\tau_p \leq \tau_s \sim L_p/C_s$, where C_s is the speed of sound. However, neither the CO_2 laser nor OPO pulse is sufficiently short to enter this limit ($\tau_s \sim 600$ ps).

To produce the depth-profiling analysis that we observe, the evaporation mechanism must be one in which only molecules near the surface of the particle evaporate at low laser energy and progressively more of the particle evaporates with increasing laser power. Within the limit of thermal confinement, though, two separate mechanisms meet these criteria. The first is pure thermal desorption, in which the molecules evaporate layer-by-layer. This is the predominant mechanism for laser fluences too low to superheat the particle and produce a phase explosion. In this case, the initial temperature of the particle following laser excitation controls the extent to which the particle evaporates before evaporative cooling effectively halts the process. Increasing the vaporization laser power increases the initial temperature and results in a more complete evaporation of the particle. We note that, for some materials, there exists a superheating regime between thermal and explosive vaporization where the superheated particle deforms and produces minimal mass loss.[25] From the perspective of this experiment, an analysis using laser powers above the deformation threshold but below the explosive vaporization threshold will behave very similarly to thermal vaporization. The second mechanism is a special case of explosive vaporization in which the light absorption is confined to a small region near the surface of the particle, as is true for a strongly absorbing material. Molecular dynamics simulations[20] show that in this case, the laser removes material in the form of vapor and nanodroplets from the illuminated surface region, leaving the unexposed portion of the particle intact. Increasing the laser power results in removal of material originating deeper in the particle. We use the term "ablation" to describe this limited-depth explosive vaporization, although it is often used more generally to refer to the mass removal of material from a substrate. Explosive vaporization arising from a uniform absorption of light over the entire particle results in what is commonly called "shattering", the breaking of the entire particle into many nanodroplets and vapor. We do not expect that such a shattering can produce the depth-profiling behavior, since it would not produce surface-specific vaporization at low laser energies.

Since both thermal desorption and ablation can qualitatively explain our observations, we must examine the laser parameters and optical properties of the particle to determine which mechanism is operative here. Ablation, as we have defined it here, requires large laser fluences and "optically thick", or strongly absorbing, particles. The conditions that favor thermal desorption are uniform heating and low laser fluence. Uniform heating requires that the particle is "optically thin" and that the diameter is small, as compared to the wavelength of the vaporization laser. In this context, "optically thin" means that the product of the particle's radius, r, and the extinction coefficient multiplied by the concentration, ϵ', satisfy the inequality, $\epsilon' r \ll 1$. Under these conditions, the laser beam is not appreciably attenuated as it passes through the particle, allowing all points inside the particle to experience the same laser fluence. The particle's diameter must be small relative to the wavelength of light to ensure that little intraparticle focusing of the evaporation laser occurs. Such focusing produces large temperature gradients and is well-known to cause the ablation of the shadow side of ~50-μm ethanol droplets irradiated with an intense CO_2 laser beam.[26]

We expect that the CO_2 laser parameters meet both of the criteria for uniform heating. On the basis of FT-IR measurements, we estimate the absolute extinction coefficient at $\lambda = 10.6$ μm for

(19) Schoolcraft, T. A.; Constable, G. S.; Zhigilei, L. V.; Garrison, B. J. *Anal. Chem.* **2000**, *72*, 5143−50.
(20) Schoolcraft, T. A.; Constable, G. S.; Jackson, B.; Zhigilei, L. V.; Garrison, B. J. *Nucl. Instrum. Methods Phys. Res., Sect. B* **2001**, *180*, 245−50.
(21) Miotello, A.; Kelly, R. *Appl. Phys. A* **1999**, *A69*, S67−S73.
(22) Zhigilei, L. V.; Garrison, B. J. *J. Appl. Phys.* **2000**, *88*, 1281−98.
(23) Yingling, Y. G.; Zhigilei, L. V.; Garrison, B. J.; Koubenakis, A.; Labrakis, J.; Georgiou, S. *Appl. Phys. Lett.* **2001**, *78*, 1631−33.
(24) Handschuh, M.; Nettesheim, S.; Zenobi, R. *App. Sur. Sci.* **1999**, *137*, 135.
(25) Latifi, H.; Xie, J.-G.; Ruekgauer, T. E.; Armstrong, R. L.; Pinnick, R. G. *Opt. Lett.* **1991**, *16*, 1129−30.
(26) Wood, C. F.; Leach, D. K.; Zhang, J.-Z.; Chang, R. K.; Barber, P. W. *Appl. Opt.* **2001**, *27*, 2279−86.

oleic acid and glycerol to be 40 and 50 mol^{-1} dm^3 cm^{-1}, respectively. These values result from measuring the spectra in a cell of known thickness (0.125 μm). Although many features saturate the detector, we can obtain absolute extinctions for weak features and can scale these values using literature spectra. We calculate only a 5% attenuation of the CO_2 laser beam as it passes through the 2-μm particle in the limit of Lambert−Beer absorption ($\epsilon' r = 0.01$). In addition, the 2-μm particle diameter is well below the CO_2 laser wavelength of 10.6 μm, making it very unlikely that internal focusing is an issue. In light of these facts, we conclude that the thermal desorption component of evaporation is responsible for the depth profiling behavior in the low-power, CO_2−VUV experiment.

As we show in Figure 6, the OPO laser exhibits a more coating-specific detection than does the CO_2 laser, indicating a difference in the evaporation conditions. Several factors may contribute to this difference. First, we tuned the wavelength of the OPO into resonance with the intense C−H stretching bands in both oleic acid and glycerol. Since this is a strong absorption band, the optical density of the particle at this wavelength is higher than for the CO_2 laser. In this case, the extinction of 350 mol^{-1} dm^3 cm^{-1} (similar for both oleic acid and glycerol) resulted in a product, ϵ'r, of ~0.1 (40% attenuation). Therefore, there is a slight gradient in the magnitude of the laser field across the diameter of the particle with a maximum at the incident face. The thermal confinement condition implies that this gradient in laser field translates into a gradient in initial temperature. If the gradient is such that the surface layers of the particle are superheated while the bulk of the particle is not, an ablative component of the vaporization may account for the increased surface-specificity of the OPO laser.

Contribution of Other Vaporization Mechanisms. Our results also show that for higher CO_2 laser fluences (>90 mJ/pulse), the vaporization step preferentially produces vapor from the core of the particle at short CO_2−VUV delays. The change in behavior is a clear indication of the contribution of a different vaporization mechanism. At sufficiently high laser fluences, the vaporization dynamics are known to move toward explosive vaporization.[19,20,25,27,28] Previous observations of this shift in vaporization dynamics have been made using a very different approach, fast photography of exploding droplets.[25,27,28] The photographic studies, although performed on larger droplets (>10 μm), confirm that above some threshold laser fluence, the particle disintegrates into a number of smaller particles and vapor,[25] a process we refer to as shattering. Although a range of laser fluences have been reported to produce this effect in a variety of systems, the fluence we used (1−10 J/cm^2) is on the same order of magnitude as those known to produce shattering.[25,29] The correlation, both qualitative and quantitative, between our observation of a change in mechanism through mass spectrometry and the same derived from photographic data gives a strong indication that our high CO_2 laser power results are a manifestation of particle shattering. In fact, we also observe a change in the internal energy distribution of the vapor molecules produced above the shattering threshold. We are currently preparing a paper that describes these results and makes more physical connections with previous observation of the laser superheating of liquid droplets. The present discussion is confined to the effect of shattering on the depth-profiling of aerosol particles.

Depending on the laser fluence, the nanoparticles created via shattering can continue to evaporate thermally, aided by further laser excitation in the case of the longer CO_2 laser pulse. Since these particles are inhomogeneous and thermal energy flow is slow on the time scale of the laser excitation, vapor voids could form in the interior of the particle at short times if the core molecules become superheated before the coating molecules. This situation could translate into a preferential detection of core molecules if the voids escape into vacuum upon shattering. At long delays, we observe the continuing thermal evaporation of the nanodroplets, likely aided by the long duration of the CO_2 laser pulse. The explanation for the short-time dynamics is speculative, though, since our FT-IR measurements are approximate and insufficient to determine the difference in heating rates between the core and coating. The important observation is that the preferential detection of core molecules suggests a change in the mechanism from a thermal, layer-by-layer desorption to an explosive vaporization.

We do not suggest that this power of 90 mJ/pulse is the threshold for producing shattering, but rather an upper limit. Since we ionize and detect only those molecules that enter the vapor phase, and since thermal desorption produces vapor preferentially from the coating, the contribution of vapor from shattering at 90 mJ/pulse must be large enough to overwhelm the component from thermal desorption to explain the preferential detection of core molecules. It is likely that in the depth-profiling regime, the shattering simply produces too little vapor to obscure the desorption component of the signal. Therefore, we expect that the mechanism can not only explain the preferential core detection but impact the depth-profiling behavior, as well. In the depth-profiling regime, we observe that even at the lowest CO_2 laser fluence that produces a detectable signal, some glycerol appears in the mass spectra. A strictly thermal desorption mechanism would not produce gas phase glycerol until nearly all the oleic acid is evaporated. Thus, a shattering component producing vapor from the core of the particle can explain the deviation of our data from the ideal thermal desorption model. The component of the short-delay signal that arises from shattering increases with increasing CO_2 laser power and dominates at high power such that the core molecules enter the vapor phase preferentially.

When the frequency of the OPO laser is resonant with the core and not the coating, we also observe preferential detection of core molecules, indicative of nonthermal vaporization. In this case, though, there is no long-delay thermal desorption component of the signal that is rich in oleic acid, as was the case for the CO_2 laser. We conclude that the particle shatters preferentially producing vapor from the core of the particle, just as for the CO_2 laser vaporization. There is no long-delay component of the desorption in this case, since the 5-ns OPO pulse does not continue to heat the nanoparticles created upon shattering. Indeed, molecular dynamics simulations of aerosol particle ablation show that the nanoparticles undergo little secondary, thermal evaporation[19,20] without continued heating.

(27) Xie, J.-G.; Ruekgauer, T. E.; Armstrong, R. L.; Pinnick, R. G. *Phys. Rev. Lett.* **1991**, *66*, 2988−91.
(28) Pinnick, R. G.; Biswas, A.; Armstrong, R. L.; Jennings, S. G.; Pendleton, J. D.; Fernandez, G. *Appl. Opt.* **1990**, *29*, 918−25.
(29) Singh, P. I.; Knight, C. J. *AIAA J.* **1980**, *18*, 96−100.

CONCLUSION

We have demonstrated a two-laser approach to single-particle mass spectrometry that provides a depth profile of heterogeneously mixed, or coated, oleic acid/glycerol particles. This result is the first such demonstration for organic constituents of aerosol particles. Using either a CO_2 laser or a tunable IR−OPO laser for vaporization, we have shown that low vaporization laser fluences result in preferential detection of the outer layers of the particles, but intermediate fluences produce mass spectra more representative of the entire particle. The CO_2 laser analysis is sensitive to changes in the coating thickness of ~10 nm for these 2-μm particles. For a particular coating thickness, the OPO laser analysis produces a higher [oleic acid]/[glycerol] ratio, indicative of more coating-specific detection. Either of these methods would be useful in identifying and categorizing single aerosol particles on the basis of the composition of the surface layers, as opposed to that of the bulk composition. Performing this analysis on a train of identical particles using several different CO_2 laser powers provides a depth profile of the particles.

The vaporization mechanism responsible for the depth-profiling ability of the CO_2 laser analysis is a thermal desorption mechanism in which the uniformly heated particle evaporates layer by layer. The OPO laser likely produces some thermal desorption flux as well; however, we attribute its increased surface-selectivity to the contribution of an ablative component of vaporization arising from the particle's larger optical density at the OPO wavelength of 3.4 μm, as well as from the laser's shorter pulse length. The latter effect will be more important for smaller (<1 μm) particles.

Particle shattering also plays a major role in the laser vaporization for high laser powers, inhibiting depth-profiling. For the CO_2 laser analysis, we found that shattering becomes the dominant mechanism near 90 mJ/pulse, producing vapor preferentially from the core of the particle followed by secondary evaporation of nanodroplets aided by the relatively long laser pulse. The OPO laser produces nonthermal desorption when the wavelength of the laser is resonant with core molecules and not coating molecules.

ACKNOWLEDGMENT

The authors gratefully acknowledge support from AFOSR, Grant F49620-99-1-0064, and DARPA, Grant F49620-98-1-0268. We would also like to thank the research group of Professor Joseph Templeton for the use of their FT-IR spectrometer.

Received for review October 12, 2001. Accepted January 17, 2002.

AC0110909